Effect of the polydispersity on the dispersion of polymers through silicas having different morphologies (fully porous and core-shell particles and monoliths)

Khac-Long Nguyen, Véronique Wernert, Renaud Denoyel

Effect of the polydispersity on the dispersion of polymers through silicas having different morphologies (fully porous and core-shell particles and monoliths)

Khac-Long Nguyen , Véronique Wernert , Renaud Denoyel

PII: S0021-9673(21)00109-6
DOI: https://doi.org/10.1016/j.chroma.2021.461985
Reference: CHROMA 461985

To appear in: *Journal of Chromatography A*

Received date: 9 December 2020
Revised date: 3 February 2021
Accepted date: 5 February 2021

Please cite this article as: Khac-Long Nguyen , Véronique Wernert , Renaud Denoyel , Effect of the polydispersity on the dispersion of polymers through silicas having different morphologies (fully porous and core-shell particles and monoliths), *Journal of Chromatography A* (2021), doi: https://doi.org/10.1016/j.chroma.2021.461985

Highlights

- Effect of polydispersity on dispersion in non adsorbing conditions is studied
- A chromatographic method for the determination of polydispersity is proposed
- Model and experimental results are comparable

Effect of the polydispersity on the dispersion of polymers through silicas having different morphologies (fully porous and core-shell particles and monoliths)

Khac-Long Nguyen[a,b], Véronique Wernert[a*], Renaud Denoyel[a]

a) Aix-Marseille Université, CNRS, MADIREL, UMR 7246, Centre Saint-Jérôme, F-13397 Marseille cedex 20, France

b) Hanoi University of Mining and Geology, 18 Vien Street, Bac Tu Liem, Hanoi, Vietnam

corresponding author:

*Véronique Wernert

Aix-Marseille Université, CNRS, MADIREL, UMR 7246, Centre Saint-Jérôme, F-13397 Marseille cedex 20, France

e-mail address: veronique.wernert@univ-amu.fr

Tel: +33 4 13 55 18 40

Abstract.

The effect of the polydispersity of polystyrenes on the dispersion through silicas having different morphologies (fully porous, core-shell particles and monoliths) was investigated. The heights equivalent to a theoretical plate (HETP) of those columns were measured for a small molecule (toluene) and a series of polystyrenes of different sizes in non-adsorbing conditions. The different contributions to the total HETP including polydispersity were determined experimentally. The longitudinal diffusion and the mass transfer resistance term were obtained from peak parking experiments. The eddy dispersion was obtained from models and experiments. The effect of polydispersity on the HETP values (H_{poly}) can thus be calculated from the total HETP by substraction of the other contributions. The results were compared to the Knox model which surestimates the H_{poly} values for porous and core-shell particles which is usually explained by an overestimation of the polydispersity index (PDI) given by the manufacturer. The PDI of two polymers (P02, M_w= 690 g.mol^{-1} and P03, M_w=1380 g.mol^{-1}) was verified by liquid chromatography by separating each fraction of the polymer on the silica columns by using adsorbing conditions which are obtained with a mixture of heptane and THF. The PDI obtained are comparable to the PDI given by the manufacturer meaning that the assumptions made by Knox are not entirely valid. A direct method is proposed in this paper in order to determine H_{poly}. In this method the excess of spreading as compared with a polymer with only one size corresponding to the average size is studied assuming the polymer size distribution is gaussian. The H_{poly} values obtained by the direct method are comparable to the experimental values.

Keywords: silica columns, polystyrenes, HETP, eddy dispersion, mass transfer mechanisms, polydispersity

1. Introduction

The transport properties of chromatographic columns are classically interpreted by the Van Deemter equation [1] relating the height to an equivalent plate (HETP) to the interstitial velocity u of the fluid:

$$HETP = A + \frac{B}{u} + Cu \quad (1)$$

This equation distinguishes three main contributions. The third one, the so-called C-term, is proportional to the velocity and represent the spreading of peaks that is due to a non-equilibrium partition of the solute concentration between the mobile phase and the stationary phase. When the mobile phase velocity increases, the rate of equilibration becomes slower, thus broadening the eluting peak. The overall mass transfer consists of the film mass transfer resistance, the adsorption-desorption kinetics, and the internal diffusion inside the mesopores. Since the convection inside particle is assumed to be negligible as compared to that outside particle, the probe in the porous particle will primarily move by molecular diffusion. This contribution to mass transfer is proportional to the velocity. When the main contribution is internal diffusion, the linearity of HETP curves versus velocity at high speed shows that the effective intraparticle diffusion is independent of velocity: it depends mainly on the pore structural properties of the stationary phase [2]. Expressions issued from the general rate model (GRM) are generally accepted and have been developed for the main structures found in chromatography: spherical particles, core shell particles and monoliths [3-8]. The second term, the so-called B-term, is inversely proportional to the velocity and represent the spreading due to the axial diffusion through the column. This diffusion occurs both in the external and internal porosities and the total diffusion coefficient D_t in the column depends on the combination of efficient diffusion coefficient around the particles (or skeleton) D_{ext} and efficient diffusion coefficient inside particles (or squeleton) D_p^{eff}. Parallel models or effective mean theories (EMT) equations are proposed to relate the three diffusion coefficients [9,10, 11]. The tortuosity of each domain is involved in the transport by diffusion process, as well as possible hydrodynamic effects between molecules and pore walls then leading to a complex phenomenon to model. *Dt* is directly accessible by peak parking experiments, whereas the determination of diffusion in external porosity and in internal porosity needs more complex approaches [10-15]. The efficient diffusion coefficient in a part of the porosity can be deduced from bulk diffusion coefficient and corresponding tortuosity. Thus, the external tortuosity can be derived from the diffusion coefficient of excluded molecules [16] or using pore blockage

approaches [17], whereas the intraparticle tortuosity needs independent methods, such as for example, the suspension dilution method [14].

The first term, the so-called A-term or eddy dispersion, was supposed to be constant in the first theories of chromatography [1] because related to the uneven repartition of flows inside the column leading to a spreading of peaks that should only depend on structure of the bed and not on the characteristics of the transported molecules. It is admitted that this term is often an intrinsic limit to the column performance and several studies were carried out to examine the role of particle size distribution, packing density and skeleton homogeneity on the amplitude of this term [18,19, 20]. Moreover, as initially developed by J.C. Giddings [21], the observed eddy dispersion cannot be fully reproduced without considering the coupling between advection and diffusion, which makes this term velocity dependent. The estimations he made of the contribution to HETP of eddy dispersion by considering variations of flows in various parts of the column are in good agreement with simulations made in last decade by the lattice-Boltzmann method for the simulation of low-Reynolds number flow of an incompressible fluid in the interparticle void space [18,19]. Nevertheless, the way this coupling occurs should again depends only on the material structure and not on the transported molecule properties. In many systems, this is what is occurs: for a given column and various molecules, the HETP curves have a nearly common minima value, which approximates the A-term, and they differ by their slope in the high velocity range because of their different affinities for the surface or their different diffusion coefficients in the porous zones. At the opposite, situations can be encountered where the HETP value is very different from a molecule to the other at the level on the minimum. This is the case, for example, when high molecular weight molecules are used [22]. In this latter study, the application of the HETP equations were applied to size exclusion chromatography, which means that the mass transfer of high molecular mass compounds was analyzed in non-adsorbing conditions. One of the main observations of this study is that the minimum of HETP curves varies strongly with mean polymer size passing through a maximum value for a polymer that have access to 25% of the porosity. The C-term follows the same trend. To explain the results, the authors introduced a contribution of polymer polydispersity to the HETP which is independent of flow rate. Formally this is a new contribution to the A-term in the Van Deemter equation. Mechanistically, despite not really described in the paper, this additional spreading could be related to several contributions: indeed, the dispersion of polymer sizes induced a distribution of retention times as well as of diffusion coefficients and one can imagine that the effect of these distributions is stronger when the considered polymer has a size close to that of mean

pore size. To assess the role of the stationary phase on these phenomena, the objective of the present paper is to address this problematic for several types of supports, fully porous spherical particles, porous-shell spherical particles and monoliths.

2. Experimental section

Chromatographic (ISEC) measurements were performed using the 1200 HPLC system (Agilent Technologies), having a quaternary gradient pump with a multi-diode array UV-VIS detector, an automatic sample injector with a 100µL loop, an autosampler and a thermostated column compartment. The injection volume was set at 1µL and all experiments were conducted at 25 °C, fixed by the column thermostat. The concentration of the solutes samples at the outlet was recorded using the diode array detector at 262 nm. The system is controlled by the Chemstation software.

Tetrahydrofuran (THF) used as a mobile phase was purchased from Carlo Erba Reagents (SDS). Toluene and heptane were purchased from Sigma-Aldrich. Twelve polystyrene standards with molecular weights Mw ranging between 162 and 1,850,000 g mol^{-1} were provided by Polymer Standards Service (Mainz, Germany). For the polymerisation of polystyrene, n-butyllithium (C_4H_9Li) is added to styrene monomer then it reacts with another styrene radical in the next step and so on. At the end of this stage, the terminating agent proton H^+ is added to remove lithium at a given time. So, the molecular weight of the polystyrenes is given by M_w=104p'+58 where p' is the number of units. Samples of toluene and polystyrenes were dissolved in the mobile phase (THF) at a concentration of 1 gL^{-1}. The characteristics of the solutes in term of diffusion coefficients and molecular sizes are given in table I. Some experiments were carried out in adsorbing conditions with the objective to separate the various fractions of a given polymer. The adsorbing conditions were obtained by using, as solvent, a mixture of THF and 3% Heptane. Several mixtures of THF and heptane have been studied with silica and the best separation of the different fractions of polystyrenes have been obtained with the mixture THF:heptane (97:3) (results not shown). Only the composition of P2 and P3 were obtained by this method.

The columns were composed of (i) fully porous particles made of silica (Lichrospher Si100, Merck), (ii) core-shell silica particles (Poroshell 120, Agilent) and (iii) monolithic silica (Chromolith, Merck). The main characteristics of the columns provided by the manufacturers are given in Table II. The particle diameter given by the manufacturer is in agreement with the mercury intrusion results in the interparticular domain. Concerning the ratio ρ of the core-shell silica particles which is the ratio between the core diameter and the

particle diameter, it is in agreement with the value deduced from porosity measurements. By assuming cylindrical pores the porous volume (V_p) is calculated from the specific surface area (S) and the pore diameter (d_p) obtained by nitrogen adsorption (V_p=S.d_p/4). The particle porosity is then calculated ($\varepsilon_p=V_p/(V_p+1/\rho_s)$ with ρ_s the particle density of silica (2.1 g/cm^3)). This particle porosity is then compared to the particle porosity obtained by nitrogen adsorption in the porous zone (ε_{pz}). Knowing that $\varepsilon_p=\varepsilon_{pz}(1-\rho^3)$, the value of ρ obtained is 0.6 which is close to the value of 0.625 given by the manufacturer.

The materials filling the columns were recently characterized by various methods [16]. The main characteristics are given in table III.

3. Results and discussion

The peak shapes obtained from all experimental tests with molecules and columns used here have a Gaussian profile. The HETP values were corrected from the dispersion in the extra-column volume [2] using the following equation:

$$HETP = L\frac{(\sigma_r^2-\sigma_i^2)}{(t_r-t_i)^2} \quad (2)$$

where σ_r^2 is the peak variance equal to the square of half of the peak width and t_r is the retention time; σ_i and t_i are the corresponding peak width and retention time with a zero-length column, respectively. The results obtained for the three columns and the ensemble of probes are given in figure 1. The observed behaviors are close to those of preceding studies [9]. For small molecules like toluene or P01, the HETP decreases with velocity then tends toward a constant value within experimental error. At low velocity spreading is governed by longitudinal diffusion whereas at high velocity eddy diffusion becomes predominant. The diffusion coefficient of these molecules is high, even inside the porous zone, and the exchange with external porosity is fast, then the C-term is small. The apparent behavior is the same for the polymers excluded from the mesoporosity, P08 to P12. The HETP is always decreasing from low velocity, where longitudinal diffusion is predominating, to high velocity where a nearly constant value (called A_{app} in the following) is observed, that could be associated to eddy diffusion. In figure 2 the HETP curves for toluene and the excluded polymers is presented for sake of comparison in the range of low HETP values. It can be observed that this apparently constant value is clearly higher for polymers than that of toluene in the case of Si100 and Poroshell, whereas the difference is small in the case of Chromolith. One can also observe that there is a difference between the various excluded polymers, with

A_{app} higher for P08 than other excluded polymers between which there are still differences but without systematic apparent behavior. A possible explanation is that interstitials pores are not accessible the same way by all the molecules. Indeed, when the total accessible porosity to a given probe is plotted as a function of molecular weight, this porosity is not exactly the same for all excluded molecules as shown in figure 3. This is due to the fact that particles at their contact points define small pores that are in the mesopore-macropore range whose accessibility varies with polymer size. This effect is less pronounced for monoliths, as shown in figure 3, where the accessible porosity versus molecular weight is apparently constant from P09 to P12 whereas it decreases slightly for Si100 and Poroshell. The curvature of monolith skeleton is less strong than that defined by contact points between spheres.

Considering now the polymers that can diffuse into the porous zone, P02 to P07, it is clear, looking at figure 1, that, when the molecular weight increases, (i) their HETP at a given velocity are shifted to higher values, (ii) pass through a maximum and (iii) then decreases. In the case of fully porous particle Si100, the behavior is similar to that described in reference [9] where the HETP, after an initial decrease corresponding to longitudinal diffusion predominance, increases linearly with velocity showing a predominance of C-term corresponding mainly here to slow intraparticle diffusion. This slope itself passes through a maximum when the polymer size increases. For Poroshell and Chromolith, the same behavior is observed but the linearity is not so good. In fact, the peaks are very sharp at high speed and after correction of extra-column spreading the error is important. For Si100 the highest HETP values and the highest slope (C-term) are obtained for P06; for Poroshell the highest HETP values are obtained for P5 and the highest C-term for P06-P07; for Chromolith the highest HETP values and the highest slope (C-term) are obtained for P04. From nitrogen adsorption (see table III), the mean mesopore sizes of Si100, Poroshell and Chromolith are 11.7 nm, 16.1 nm and 16.1 nm, respectively, whereas the diameters (table I) of P06, P05 and P04 are 7.2, 4.7 and 3.0 nm, respectively. There is then no correlation between average pore size and the transport behavior: the presence of the maximum described above which shows a higher resistance to mass transfer for a given polymer size is probably related to the ratio probe size/pore size but from a material to the other the maximum is not obtained for the same ratio. The pore size distribution and the pore organization play certainly a role in this behavior.

In the low velocity range, the behavior of Si100 is different from the two other samples. The decreasing part of the HETP at low velocities is visible only for toluene and the very large polymers. For all polymers diffusing inside mesopores, the HETP lowest value is the first measured. This effect is also visible for P04 and P05 in the case of Poroshell. For Chromolith

the initial decreasing part of HETP versus velocity is visible for all probes. Smaller velocities cannot be tested because of instrumental limitations. This shows that in some cases the spreading by longitudinal diffusion is so small that its contribution to HETP is not visible, *i.e.* is less visible than other contributions. A possible explanation is that another important contribution is added to the HETP due to the polydispersity of the polymers, as suggested in [9]. These authors suppose a constant contribution, H_{poly}, for each polymer independent of velocity. After fitting their HETP data with standard equations, they logically deduced that H_{poly} passed through a maximum as a function of polymer size. Clearly, the present results show that this contribution also depends on the stationary phase. At a first glance, the way the polymer polydispersity may affect the spreading of peaks is that each polymer size composing the polydispersed polymer sample has its own retention time and diffusion coefficient: there is then a distribution of retention times and diffusion coefficients for each polydispersed polymer sample. This problem of the incidence of polydispersity in the determination of the true plate height has been addressed for example by Knox et al [22]. After considering a gaussian distribution of polymer lengths, they derive the following expression for the peak variance resulting from polydispersity of the sample, σ^2_{poly}:

$$\sigma^2_{poly} = S^2\,(P-1)(1+\alpha) \tag{3}$$

where: - P is the polydispersity index (PDI) given in Table I for each sample,

- α is a correction term, expressed by:

$$\alpha = \frac{11}{4}(P-1) + \frac{137}{12}(P-1)^2 \tag{4}$$

- S is the negative reciprocal of the slope of the calibration curve of *ln(Mw)* versus mean retention time. These curves are given in figure 4 at a flow rate of 0.5mL.min^{-1}. The calculations made using equation (3) and:

$$H_{poly} = L\frac{\sigma^2_{poly}}{t_r^2} \tag{5}$$

give the values of H_{poly} reported in table IV. It is clear that in most cases, the H_{poly} value is higher than the HETP value, excepted in the case of Chromolith. This shows that this approach overestimates this contribution as already underlined [23]. One of the invoked reasons was that the PDI of the polymers provided by the manufacturer are overestimated, which leads to large variations of *(P-1)* term in equation (3). However, the H_{poly} values for a given polymer are different from a sample to the other, which means that the origin of H_{poly} large values is also due to *S* in equation (3), which depends on the material.

Another possibility based on equation (3) to evaluate H_{poly}, is to try to obtain the PDI from an independent method. For example, in [23], mass spectrometry (MALDI-TOF-MS) was used to determine the PDI of some polystyrenes and effectively the results shown that the PDIs were smaller than that expected from manufacturer data. In this paper [23], the interpretation of data was made by using equation (3) which assumes that spreading due to polydispersity is simply additive to other contributions of spreading, which is only true if they are independent phenomena.

If the composition of the polymer sample is known, the calculation of the H_{poly} contribution can be made by directly summing the gaussian contributions of all fractions constituting the polymer sample. To do that it is necessary to know the composition of the considered polymer. This was made possible here by carrying out experiments in adsorbing conditions. This is shown in figure 5, where the chromatograms of P02 and P03 on Si100 and Poroshell, respectively, in a mixture THF/heptane evidence the various fractions of polystyrene. For polystyrenes with a larger molecular weight, the adsorption was too strong, and the chromatograms cannot be recorded in a reasonable time. In fact, adsorption affinity of polystyrenes for the silica surface increases with the number of units p of the polystyrenes, as generally observed in polymer adsorption studies [24]. P02 and P03 have 10 and 14 fractions, respectively. From these chromatograms, it is possible to recalculate the weight composition of the polymer and the PDI: 1.07 and 1.08 are obtained for P02 and P03, respectively, values that are close to those of manufacturer (table I). The chromatogram obtained for a given polystyrene sample (P02 or P03) can be fitted by one Gauss function or by the sum of n Gauss functions, each corresponding to one of the fractions which are present in P02 or P03 samples. The absorbance versus time is then given by:

$$y = \sum_{i=1}^{n} \frac{A_i}{w\sqrt{\pi/2}} e^{-2\left(\frac{t-t_{r,i}}{w}\right)^2} \quad (6)$$

where:

- t is the time,
- A_i is the area of the peak of fraction i,
- $t_{r,i}$ is the mean retention time of fraction i,
- n is the number of fractions in the polystyrene sample,
- w is the peak width of the chromatogram of each fraction supposed to be the same for all fractions.

The mean retention time of each fraction, $t_{r,i}$, is obtained by fitting the curve of mean retention time versus molecular weight that is obtained for each polymer (Fig. 4). In the case of P02, the number of fractions is assumed to be 10. The first fraction has 3 units of styrene, the second fraction has 4 units of styrene and so on. From the chromatogram of P02 with 10 fractions, the percentages of mass for each fraction are obtained. The retention time of each fraction in the solvent THF is calculated by the equations fitting the data of Fig. 4. By using the Gauss function to fit the experimental data, one obtains retention time, area and width of the peak. From peak area and the weight composition, the area of each fraction A_i is evaluated. By using the Solver function in Excel, the width of each fraction w is obtained by adjusting experimental data with equation 5. Figure 6 shows the experimental peak of the polymer P02, the gaussian peak fitting it, the peak sum of all fractions and the peaks of some fractions given by Gauss function with corresponding A_i and w (for 3,6, and 9 units). Finally, the contribution of polydispersity is given by the difference between the measured variance and the variance calculated for one fraction from the value w in equation (5). The deduced h_{poly} and H_{poly} are given in table V, column "direct method".

The value of H_{poly} can be also deduced directly from the HETP values by considering the method generally used in the literature that will be called here "substraction method" and detailed hereafter. The B-term is evaluated from peak parking experiments, the C-term from the slope of HETP versus velocity in the linear range at high velocity, which enables to extract the contribution of eddy diffusion and polydispersity following (in reduced form):

$$h_{eddy}+\mathrm{h}_{poly} = \square - \frac{b}{v} - cv \qquad (7)$$

where h is the reduced experimental HETP data (HETP divided by porous domain size), b and c are the reduced longitudinal diffusion and mass transfer terms (B and C terms divided by porous domain size), respectively. The values of b and c could be obtained in dynamic conditions by fitting the HETP curve with the van Deemter equation or in static conditions by using the peak parking method. In this study, the b and c values are obtained from peak parking experiments which are presented in a paper published previously [16]. The h_{eddy} term is the more complex to evaluate. Using the coupling theory of Giddings [21] that was later confirmed by simulations [18,19], the eddy dispersion term is:

$$h_{eddy} = \sum_{i=1}^{4} \frac{2\lambda_i}{1+(\frac{2\lambda_i}{\omega_i})v^{-1}} \qquad (8)$$

This term has four contributions: trans-channel, short range interchannel, long range interchannel and trans-column. λ_i and ω_i are structural parameters characterizing each contribution. According to Giddings, the main velocity bias in liquid chromatography are the trans-channel (i=1), the short-range inter-channel (i=2) and the trans-column (i=3). The two first contribution terms could be obtained from simulation. The trans-column term is more difficult to obtain because it results from a complex combination of the radial velocity contribution. This term can be estimated by substracting the first two terms from the overall eddy diffusion term [25, 26]. The values of λ_i and ω_i given by Giddings are λ_1=0.5, ω_1=0.01, λ_2=0.5 and ω_2=0.5. Today, these values are still qualitatively valid [27]. Those values have been verified by simulations [19]. The values taken in this study for spherical porous particles comes from [19] (λ_1=0.45, ω_1=0.0041, λ_2=0.23 and ω_2=0.13 for Si100 and λ_1=0.45, ω_1=0.0045, λ_2=0.25 and ω_2=0.13 for porous-shell particles). The values are a little different because the external porosities of those columns are slightly different.

For the monolithic column the long range interchannel is also negligible [28]. The values of λ_i and ω_i for the transchannel and short range interchannel are taken from [28] (ω_1=0.0104, λ_2=0.3633, ω_2=0.2034). The transchannel eddy dispersion contribution $h_{eddy,1}$ is represented by a simple velocity-proportional term. The parameters are obtained by pore-scale simulations of flow and dispersion by using the morphology reconstruction obtained by confocal laser scanning microscopy. The values of those contributions represent less than 5% of the overall HETP values. Similar results have been obtained by [29].

The trans-column term (h_{TC}), assumed to be the same for all molecules, could be calculated from the HETP value at high speed for the molecules that are fully excluded from porous zones (P10 to P12) and for which the contribution of polydispersity is low (see discussion above):

$$h_{TC} = h_{eddy} - h_{TS} - h_{IC} \quad (9)$$

Nevertheless, looking at results in this velocity domain in figure 2, HETP values are dispersed and different from an excluded polymer (P09 to P12) to the other without any clear correlation. Moreover, the HETP value of toluene, despite it contains intraparticle diffusion components, is smaller than that of excluded polymers and is more accurately determined. Consequently, toluene results were used to calculate the trans-column term by equation (9).

The h_{poly} values for P02 and P03 are then calculated according to $h_{poly}=h_{eddy}-h_{TS}-h_{IC}-h_{TC}$. The mean values of h_{poly} thus calculated are reported in table V in the column "substraction method".

For Poroshell and Chromolith the agreement between the two methods is reasonable whereas the difference between the two methods is large for Si100. This may be due to the structure of Si100 which present an eddy term around twice that of Poroshell despite both are spherical stationary phases with close particle diameters. As shown by mercury porosimetry, the pore structure of Si100 seems more complex than that of Poroshell. The mesopore range in Si100 column is indeed very large [16] and maybe there is, for example, a different particle roughness that could affect eddy diffusion. Another interesting point is the comparison of data of tables V and IV. As already underlined, the H_{poly} derived from equation (3) are very high, but the reason is not an overestimated value of PDI since the method used here to determine the PDI of P02 and P03 gives values similar to that of the manufacturer used in the calculation of table IV. A possible reason is that the hypotheses used to derive equation (3) are not entirely correct. Indeed, this derivation assumes that the variance of the polymer size distribution is simply added to the other variances due to spreading by diffusion, advection etc…

In order to check this assumption, a generalization of the "direct method" is proposed in the following. In fact, what is looked for is the excess of spreading as compared with a polymer with only one size corresponding to the average size. If the polymer size distribution is assumed to be gaussian, the equation (6) can be rewritten:

$$y = \sum_{i=1}^{n} \frac{k.e^{-2\left(\frac{i-\bar{n}}{w_p}\right)^2}}{w_p\sqrt{\pi/2}} \frac{e^{-2\left(\frac{t-t_{r,i}}{w}\right)^2}}{w\sqrt{\pi/2}} \quad (10)$$

Where k is a constant related to the total amount of polymer in the injected sample, w_p the width of the polymer size distribution and $\bar{n}$ the center of the polymer size distribution. The number of units i is used in equation (10) instead of molecular weights because of the linear relation between them ($M_{p,i}=104i+58$). The PDI is the ratio between M_p and M_n. M_p is the mean molecular weight value given by the manufacturer. M_n is calculated by equation (11):

$$M_n = \frac{\sum_{i=1}^{n} M_{p,i}.N_i}{\sum_{i=1}^{n} N_i} \quad (11)$$

where N_i is the number of molecules in fraction i given by equation (12):

$$N_i = \frac{k.e^{-2\left(\frac{i-\bar{n}}{w_p}\right)^2}}{w_p\sqrt{\frac{\pi}{2}}}\frac{N_a}{M_{p,i}} \quad (12)$$

where N_a is the Avogadro Number. The value of w_p is calculated so that the calculated PDI is equal to the manufacturer PDI. The value of w is taken from the experiment with the monomer because the A term for this molecule is supposed to be independent of any polydispersity effect or size effect.

Then the chromatogram obtained from equation (10) is adjusted by only one gaussian curve attributed to polymer of size $\bar{n}$ with simulated width w_d:

$$y = \frac{k.e^{-2\left(\frac{t-t_{r,\bar{n}}}{w_d}\right)^2}}{w_d\sqrt{\pi/2}} \quad (13)$$

The HETP is calculated with $t_{r,\bar{n}}$ and w_d. H_{poly} is then obtained by substracting HP1 (direct method).

Field Code Changed

The results of the calculations are presented in figure 7, where are plotted (i) the HETP experimental value of the polymer to which the A value of the monomer has been substracted H-HP1, (ii) the HETP contribution to polydispersity H_{poly} derived from the Knox equation (3) and (iii) the one obtained by fitting chromatograms with equation (13) (direct method). As already observed in the case of P02 and P03, the *Hpoly* value obtained by the direct method is the closest from the experimental one. It means that the direct method is more suitable to describe the influence of polydispersity on peak spreading than the Knox model using the same PDI. As indicated above, the Knox model assume that the variance of the polymer distribution can be simply added to the other variances related to spreading, which statistically significates that the influence of polymer polydispersity is a phenomenon which is independent of the others. This is probably an approximation because the position of the peak of one of the polymers constituting the polymer mixture on the time scale is not at random as compared to the other polymers of the mixture: these positions are defined by the relationship between molecular weight and retention time. When events are not independent, variances are not additives. Another information brought by these comparisons is that the PDI given by the manufacturer are not very far from the actual one.

Credit Author statement

Khac Long Nguyen : methodology, writing, Véronique Wernert : methodology, writing, reviewing and editing, Renaud Denoyel : methodology, writing, reviewing and editing, supervision

Declaration of Competing Interest

The authors declare that they have no known competing financial interests or personal relationships that could have appeared to influence the work reported in this paper.

Acknowledgments

The authors thanks ANR french agency, Project ANR-TAMTAM N° ANR-15-CE08-0008-01 and Vietnam Ministry of Education and Training for financial support.

References

[1] J.J. van Deemter, F.J. Zuiderweg, A. Klinkenberg, Longitudinal diffusion and resistance to mass transfer as causes of nonideality in chromatography, Chemical Engineering Science. 5 (1956) 271–289. doi:10.1016/0009-2509(56)80003-1.

[2] F. Gritti, G. Guiochon, Impact of retention on trans-column velocity biases in packed columns, AIChE Journal. 56 (2010) 1495–1509. doi:10.1002/aic.12074.

[3] E. Kucera, J. Chromatogr. 19 (1965) 237.

[4] K. Miyabe, Moment theory for kinetic study of chromatography, TrAC Trends in Analytical Chemistry. 81 (2016) 79–86. doi:10.1016/j.trac.2016.01.003.

[5] K. Miyabe, G. Guiochon, The Moment Equations of Chromatography for Monolithic Stationary Phases, J. Phys. Chem. B. 106 (2002) 8898–8909. doi:10.1021/jp020555b.

[6] K. Miyabe, New Moment Equations for Chromatography Using Various Stationary Phases of Different Structural Characteristics, Anal. Chem. 79 (2007) 7457–7472. doi:10.1021/ac070825s.

[7] K. Miyabe, Evaluation of chromatographic performance of various packing materials having different structural characteristics as stationary phase for fast high performance liquid chromatography by new moment equations, Journal of Chromatography A. 1183 (2008) 49–64. doi:10.1016/j.chroma.2007.12.064.

[8] K. Miyabe, Moment Equations for Chromatography Using Superficially Porous Spherical Particles, Analytical Sciences. 27 (2011) 1007–1007. doi:10.2116/analsci.27.1007.

[9] F. Gritti, G. Guiochon, Application of the General Height Equivalent to a Theoretical Plate Equation to Size Exclusion Chromatography. Study of the Mass Transfer of High-Molecular-Mass Compounds in Liquid Chromatography, Anal. Chem. 79 (2007) 3188–3198. doi:10.1021/ac0623742.

[10] G. Desmet, S. Deridder, Effective medium theory expressions for the effective diffusion in chromatographic beds filled with porous, non-porous and porous-shell particles and cylinders. Part I: Theory, Journal of Chromatography A. 1218 (2011) 32–45. doi:10.1016/j.chroma.2010.10.087.

[11] V. Wernert, R. Bouchet, R. Denoyel, Impact of the solute exclusion on the bed longitudinal diffusion coefficient and particle intra-tortuosity determined by ISEC, Journal of Chromatography A. 1325 (2014) 179–185. doi:10.1016/j.chroma.2013.12.029.

[12] E.M. Renkin, Filtration, diffusion, and molecular sieving through porous cellulose membranes, J. Gen. Physiol. 38 (1954) 225–243.

[13] V. Wernert, R. Bouchet, R. Denoyel, Influence of Molecule Size on Its Transport Properties through a Porous Medium, Anal. Chem. 82 (2010) 2668–2679. doi:10.1021/ac902858b.

[14] M. Barrande, R. Bouchet, R. Denoyel, Tortuosity of Porous Particles, Anal. Chem. 79 (2007) 9115–9121. doi:10.1021/ac071377r.

[15] F. Gritti, G. Guiochon, Mass transfer kinetics, band broadening and column efficiency, Journal of Chromatography A. 1221 (2012) 2–40. doi:10.1016/j.chroma.2011.04.058

[16] K.L. Nguyen, V. Wernert, A. Morgado Lopes, L. Sorbier, R. Denoyel, Effect of tortuosity on diffusion of polystyrenes through chromatographic columns filled with fully porous and porous-shell particles and monoliths, Mic. Mes. Mat. 293 (2020) 109776. https://doi.org/10.1016/j.micromeso.2019.109776

[17] F. Gritti and G. Guiochon, Impact of Retention on Trans-Column Velocity Biases in Packed Columns, AICHE Journal, 56 (2010) 1495-1509.

[18] A. Daneyko, A. Höltzel, S. Khirevich, U. Tallarek, Influence of the Particle Size Distribution on Hydraulic Permeability and Eddy Dispersion in Bulk Packings, Anal. Chem. 83 (2011) 3903–3910. doi:10.1021/ac200424p.

[19] S. Khirevich, A. Daneyko, A. Höltzel, A. Seidel-Morgenstern, U. Tallarek, Statistical analysis of packed beds, the origin of short-range disorder, and its impact on eddy dispersion, Journal of Chromatography A. 1217 (2010) 4713–4722. doi:10.1016/j.chroma.2010.05.019.

[20] K. Hormann, U. Tallarek, Analytical silica monoliths with submicron macropores: Current limitations to a direct morphology–column efficiency scaling, Journal of Chromatography A., 1312 (2013) 26– 36. doi:10.1016/j.chroma.2013.08.087

[21] J.C. Giddings, Dynamics of chromatography, M. Dekker, New York, 1965.

[22] J.H. Knox, F. McLennan, Allowance for polydispersity in the determination of the true plate height in GPC, Chromatographia. 10 (1977) 75–78. doi:10.1007/BF02274463.

[23] Y. Vander Heyden, S.-T. Popovici, B.B.P. Staal, P.J. Schoenmakers, Contribution of the polymer standards' polydispersity to the observed band broadening in size-exclusion chromatography, J. Chromatogr. A. 986 (2003) 1–15. doi:10.1016/S0021-9673(02)01957-X

[24] P. Trens, R. Denoyel, Conformation of Poly(Ethylene Glycol) Polymers at the Silica Water Interface - A Microcalorimetric Study, Langmuir 9 (1993) 519-522.

[25] F. Gritti, G. Guiochon, Relationship between trans-column eddy diffusion and retention in liquid chromatography: Theory and experimental evidence, J. Chromatogr. A. 1217 (2010) 6350–6365. doi:10.1016/j.chroma.2010.07.029.

[26] F. Gritti, G. Guiochon, Measurement of the eddy dispersion term in chromatographic columns. II. Application to new prototypes of 2.3 and 3.2 mm I.D. monolithic silica columns, J. Chromatogr. A. 1227 (2012) 82–95. doi:10.1016/j.chroma.2011.12.065.

[27] F., I. Leonardis, J. Abia, G. Guiochon, Physical properties and structure of fine core–shell particles used as packing materials for chromatography: Relationships between particle characteristics and column performance, J. Chromatogr. A. 1217 (2010) 3819–3843. doi:10.1016/j.chroma.2010.04.026.

[28] D. Hlushkou, K. Hormann, A. Höltzel, S. Khirevich, A. Seidel-Morgenstern, U. Tallarek, Comparison of first- and second-generation analytical silica monoliths by pore-scale simulations of eddy dispersion in the bulk region, J. Chromatogr. A 57 (2018) 3031–3042. https://doi.org/10.1016/j.chroma.2013.06.039

[29] F. Gritti, G. Guiochon, Measurement of the eddy diffusion term in chromatographic columns. I. Application to the first generation of 4.6 mm I.D. monolithic columns, J. Chromatogr. A. 1218 (2011) 5216–5227. doi:10.1016/j.chroma.2011.05.101.

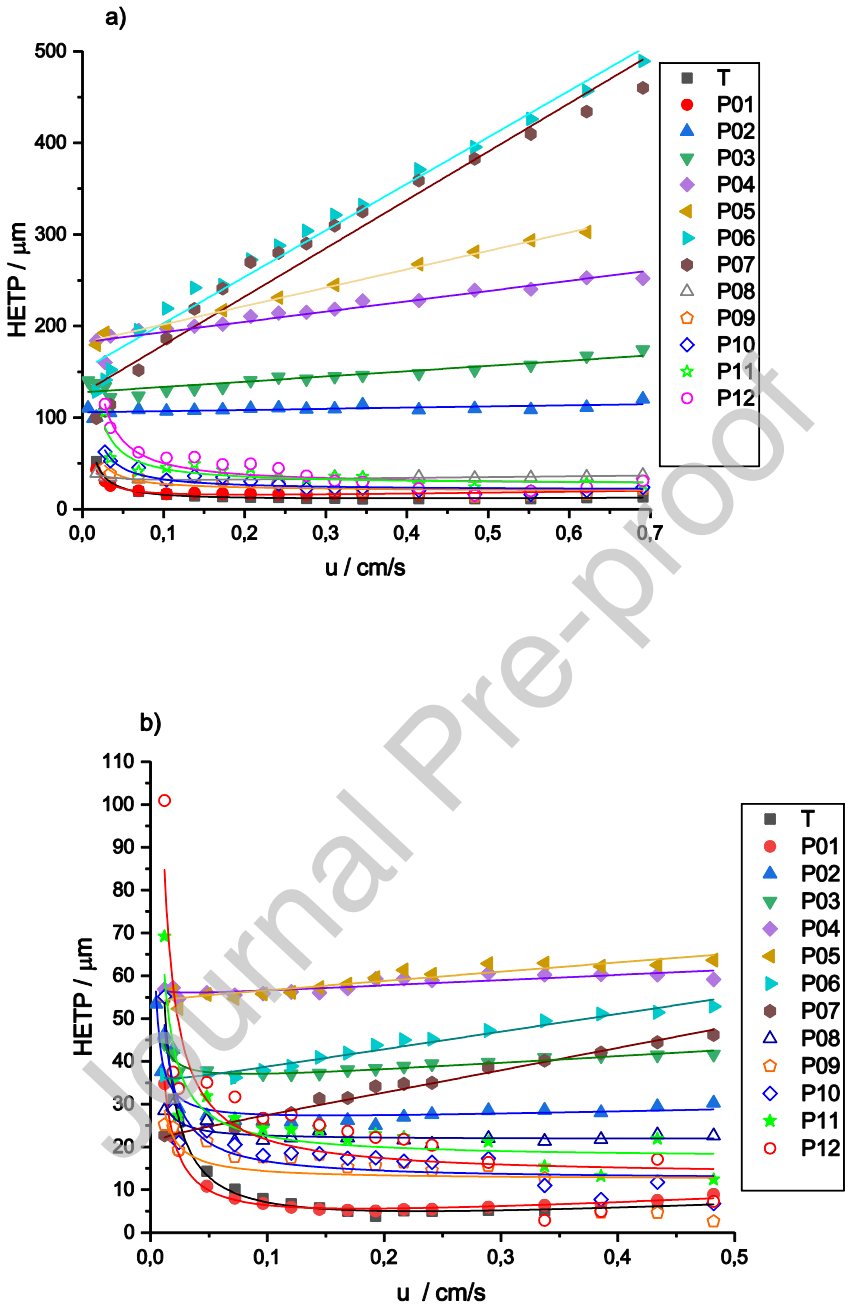

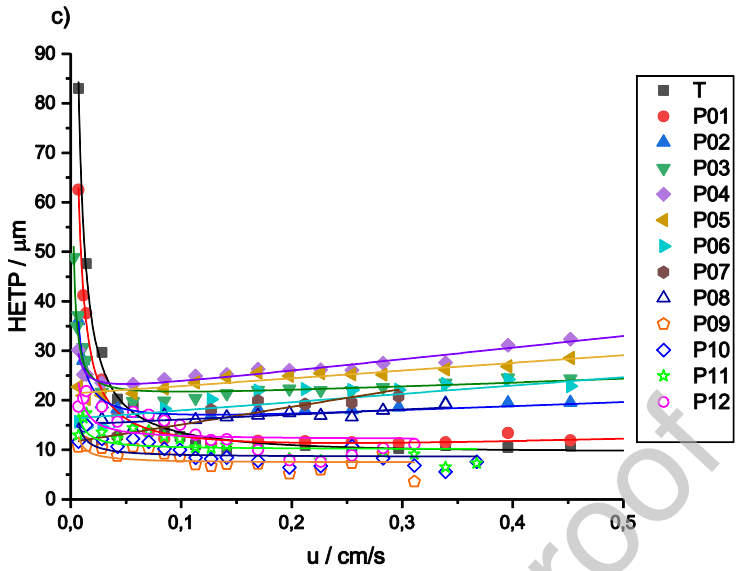

Figure 1: Corrected HETP of molecules as a function of interstitial velocity through a) Si 100 b) Poroshell and c) Chromolith columns. Lines: fit with the van Deemter equation.

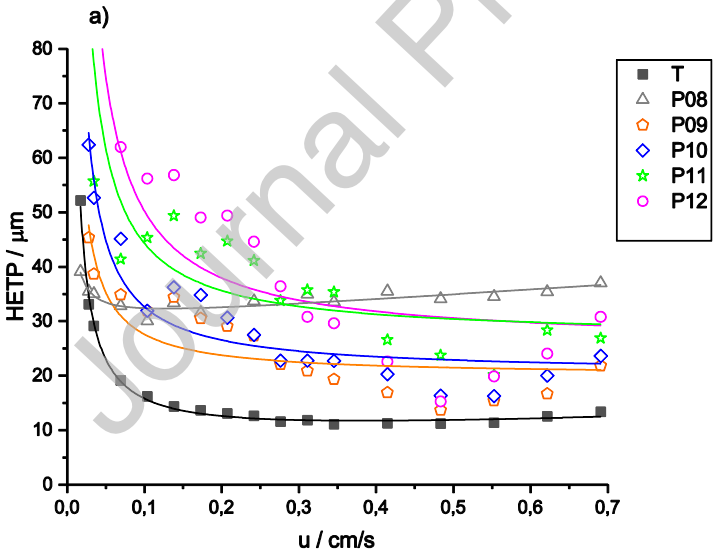

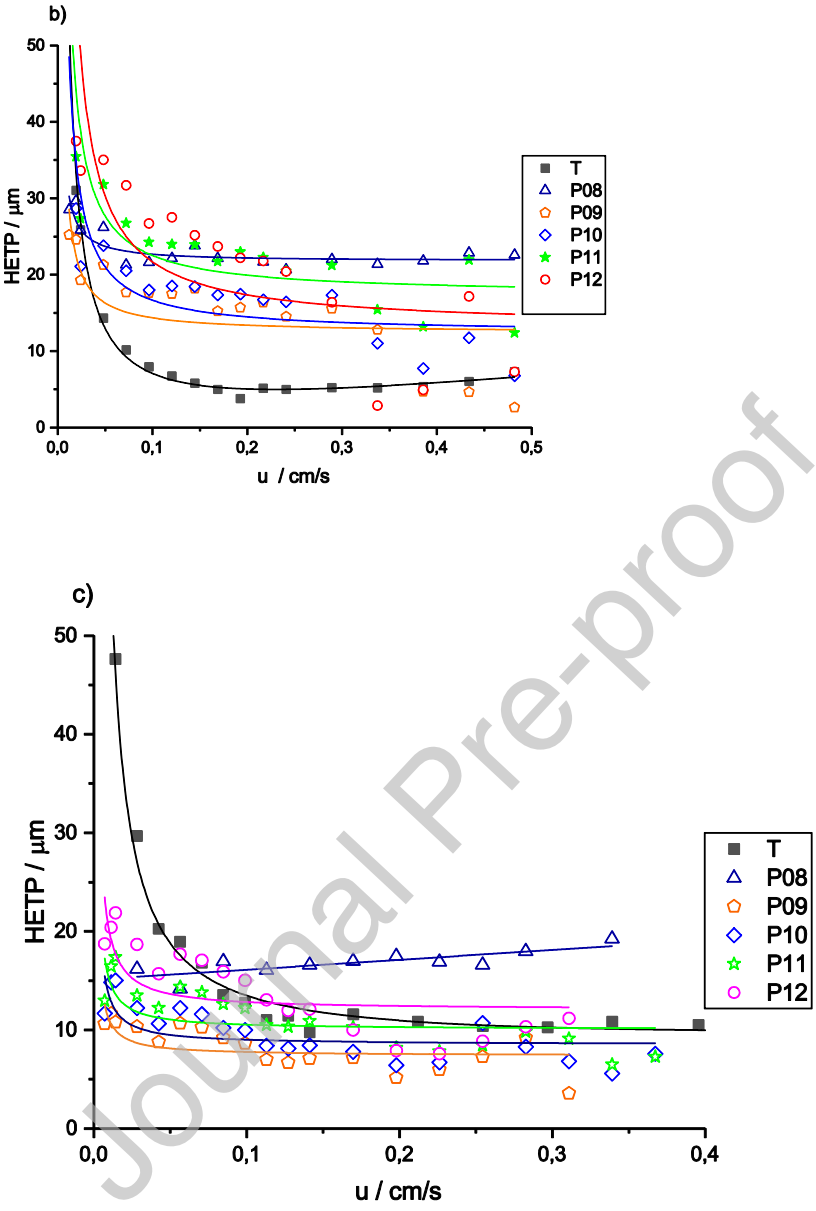

Figure 2. Corrected HETP of small and excluded molecules as a function of interstitial velocity through a) Si 100 b) Poroshell and c) Chromolith columns. Lines: fit with the van Deemter equation.

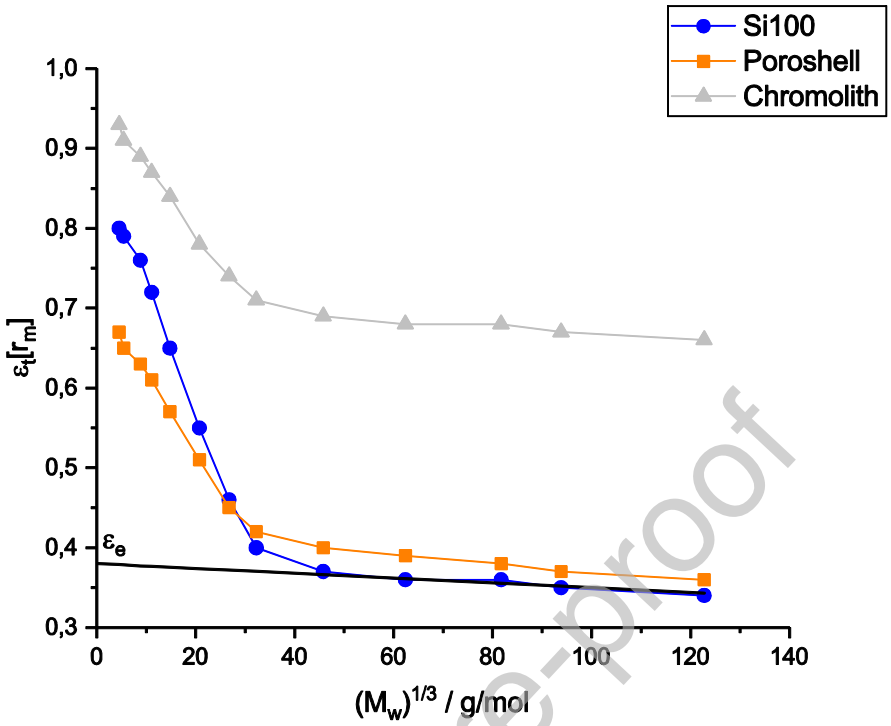

Figure 3. Total porosity of polystyrenes as a function of the cubic root of the molecular weight of the polystyrenes for Si 100, Poroshell and Chromolith columns.

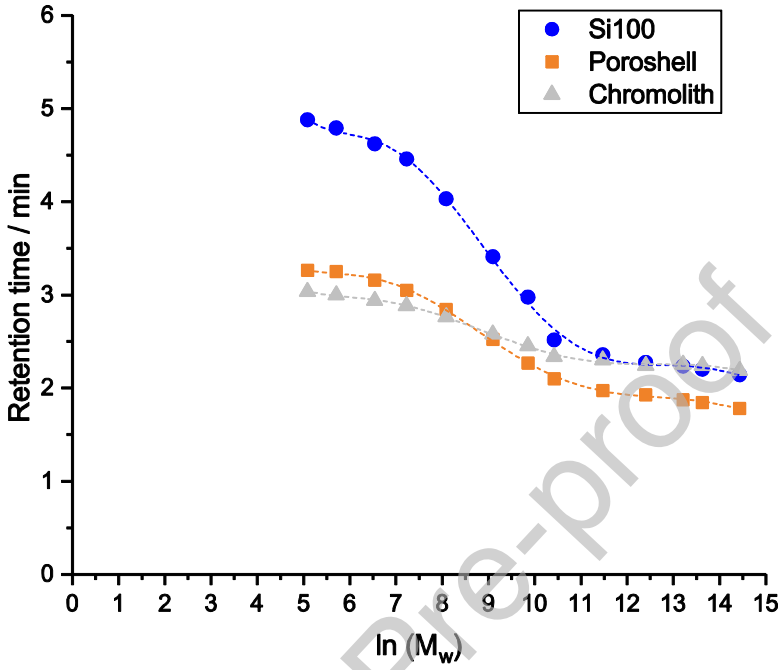

Figure 4. Calibration curve of the retention time as a function of molecular weight at a flow rate of 0.5mL.min^{-1} for Si100 (discs) Poroshell (squares) and Chromolith (triangles). Lines are equations used to fit the data.

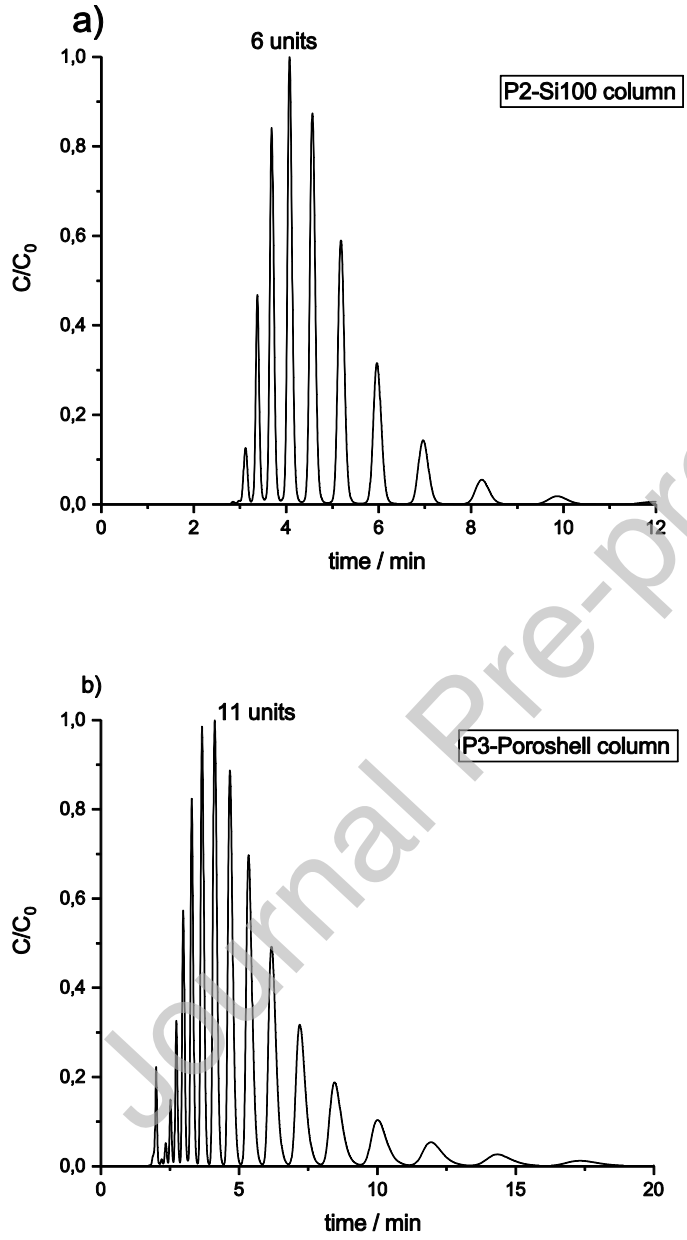

Figure 5. Chromatograms obtained for polystyrenes in the mixture of n-heptane and THF at the flow rate of 1ml.min^{-1} a) P2 with Si 100 column and b) P3 with Poroshell column.

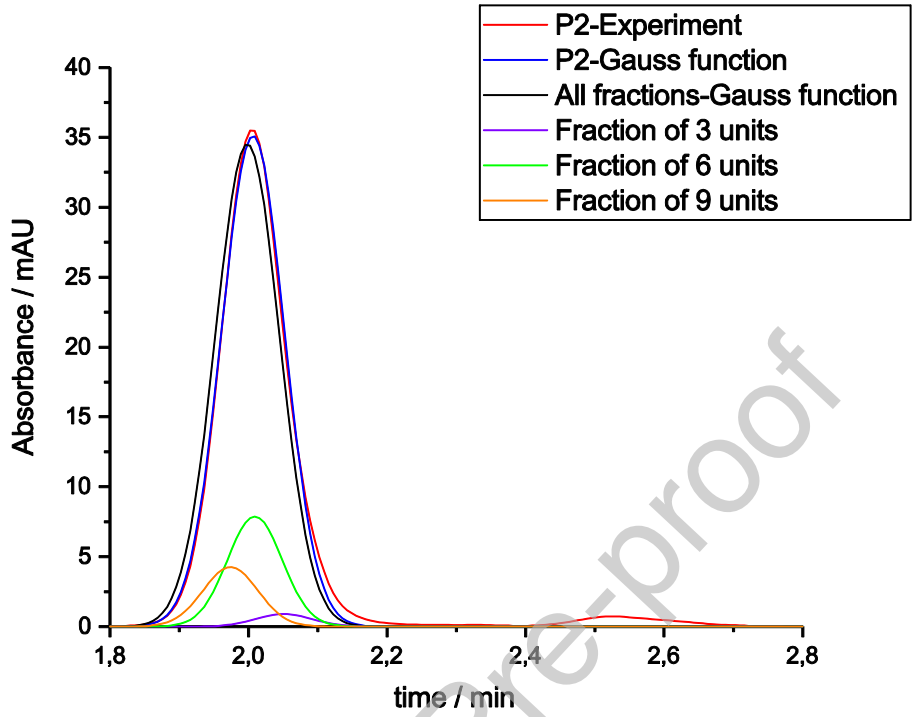

Figure 6. Chromatograms of P2 and different fractions of P2 having different number of units at 1.2 ml.min^{-1} through Si 100 column.

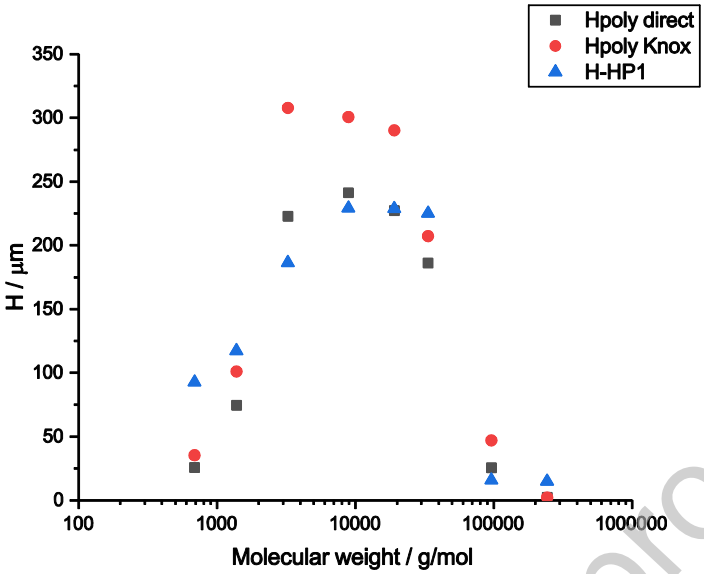

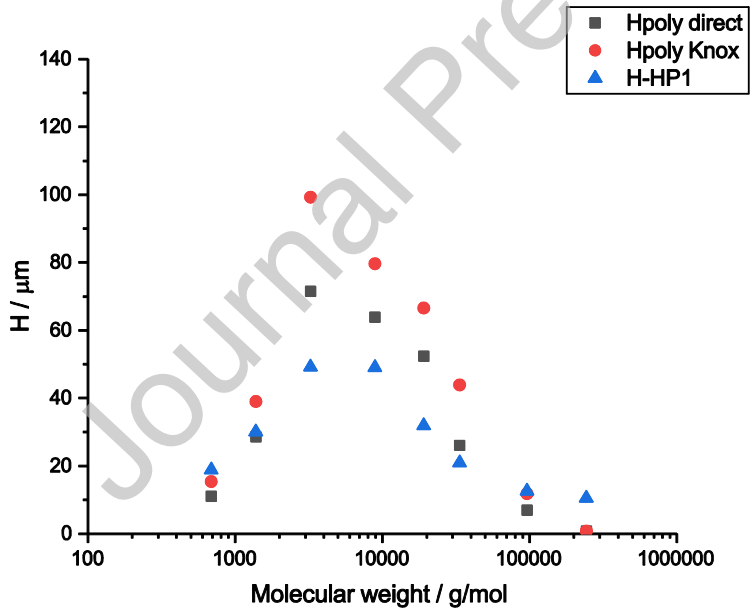

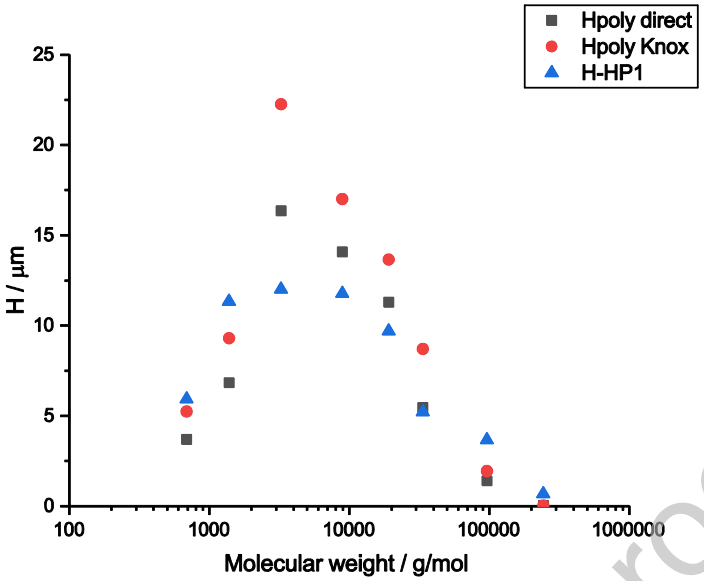

Figure 7: HETP experimental value of the polymer to which the A value of the monomer has been substracted *H-HP1*, HETP contribution to polydispersity *Hpoly* derived from the Knox equation and H_{poly} obtained by the direct method. Si100 (a), Poroshell (b), Chromolith (c).

Table I. Molecular weights (Mw), polydispersity (PDI), bulk diffusion coefficient D_m obtained by TDA for the smallest polymers (Toluene, P01, P02 and P03) and by DLS for the others polymers (P04 to P12) of the solutes used in ISEC and hydrodynamic radii r_m calculated with Stokes Einstein equation. The solvent is THF and the temperature is 298 K.

Polymer code	Molecular weight M_w [(1)] /g mol^{-1}	PDI[(1)]	Molecular diffusion coefficient D_m (TDA and DLS measurements) /m^{2}s^{-1}	probe radius r_m /nm
toluene	92		$(2.35\pm0.11).10^{-9}$	0.205±0.009
P01	162	1.00	$(1.85\pm0.11).10^{-9}$	0.26±0.02
P02	690	1.09	$(7.09\pm0.20).10^{-10}$	0.68±0.02
P03	1380	1.05	$(5.16\pm0.21).10^{-10}$	0.93±0.04
P04	3250	1.05	$(3.21\pm0.28).10^{-10}$ (2)	1.50±0.13 (2)
P05	8900	1.03	$(2.036\pm0.005).10^{-10}$ (2)	2.36±0.01 (2)
P06	19100	1.03	$(1.327\pm0.006).10^{-10}$ (2)	3.62±0.02 (2)
P07	33500	1.03	$(8.520\pm0.005).10^{-11}$ (2)	5.633±0.004 (2)
P08	96000	1.04	$(5.083\pm0.008).10^{-11}$ (2)	9.44±0.02 (2)
P09	243000	1.03	$(3.194\pm0.009).10^{-11}$ (2)	15.02±0.04 (2)
P10	546000	1.02	$(2.101\pm0.009).10^{-11}$ (2)	22.84±0.10 (2)
P11	827000	1.08	$(1.650\pm0.008).10^{-11}$ (2)	29.09±0.15 (2)
P12	1850000	1.05	$(1.12\pm0.01).10^{-11}$ (2)	42.90±0.40 (2)

(1) Given by supplier (2) Nguyen *et al* 2020 [16]

Table II : Geometrical characteristics of the considered columns, including the column's dimension, particle diameter d'_p, the ratio ρ between the diameter of the core d_c and the diameter of the particle and the mean pore diameter (d_p) (data taken form manufacturers documentation)

	Samples	Suppliers	Support	Column's dimension length [mm] I.D. [mm]	d'_p (µm)	$\rho=d_{core}/d'_p$	d_p (nm)
Totally porous particles	Lichrospher Si 100	Merck	silica	250x4	5	0	10
Core-shell particles	Poroshell 120	Agilent	silica	150x4.6	4	0.625	12
Monoliths	Chromolith Si	Merck	silica	100x4.6	1 (skeleton size)	0	13

Table III. Structural properties of the columns including the total porosity ε_t, the external porosity ε_e, the porosity of the porous zone ε_{pz} and the pore diameter (d_p) obtained by ISEC, mercury intrusion porosimetry and N_2 adsorption. The macropore diameter is obtained by Hg porosimetry (data from Ref [16]).

Materials	ISEC				Hg porosimetry					N_2 adsorption (NLDFT)		
	ε_t	ε_e	ε_{pz}	d_p (nm)	ε_t	ε_e	ε_{pz}	d_p (nm)	d_{macro} (µm)	ε_{pz}	d_p (nm)	a_s m^2/g
Lichrospher	0.80	0.38	0.68	14.2	0.77	0.36	0.64	6.5 and 17	2.21	0.73	11.68	426
Poroshell	0.67	0.42	0.57	13.3	0.62	0.37	0.53	11.8	1.05	0.68	16.09	136
Chromolith	0.92	0.71	0.72	11.7	0.87	0.63	0.65	12.0	1.77	0.68	16.09	276

Table IV. HETP and H_{poly} derived from Knox model for the polymers in the different chromatographic columns at 0.5ml.min^{-1}

Polymer	PDI	Si 100		Poroshell		Chromolith	
		Hpoly, µm	HETP, µm	Hpoly, µm	HETP, µm	Hpoly, µm	HETP, µm
P2	1.09	35.2	108.3	15.4	25.9	5.2	15.5
P3	1.05	100.9	132.9	39.0	37.1	9.3	20.9
P4	1.05	307.7	202.0	99.2	56.2	22.2	21.6
P5	1.03	300.6	244.8	79.6	56.1	17.0	21.4
P6	1.03	289.9	244.3	66.5	38.8	13.6	19.3
P7	1.03	206.8	240.7	43.8	27.9	8.7	14.8
P8	1.04	46.9	31.5	11.8	19.6	1.9	13.3
P9	1.03	2.2	30.5	0.8	17.5	0.0	10.3

Table V: h_{poly} and H_{poly} (between paranthesis) for P2 and P3 determined by substraction method or direct method

Sample	Si 100 column		Poroshell column		Chromolith column	
	Substraction method	Direct method	Substraction method	Direct method	Substraction method	Direct method
P2	19±1 (97±4)	6.0 (30)	5.7±0.2 (23±1)	1.7 (8.5)	7±2 (7±2)	3.8 (3.8)
P3	26±2 (129±11)	9.8 (50)	8.6±0.2 (34±1)	5.7 (22.8)	12±3 (12±3)	7.1 (7.1)